PERGAMON

Organic Geochemistry 31 (2000) 1041–1052

Organic Geochemistry

www.elsevier.nl/locate/orggeochem

Investigation of thermal maturity of lower Palaeozoic hydrocarbon source rocks by means of vitrinite-like maceral reflectance — a Tarim Basin case study

Xiao Xianming [a,*], R.W.T. Wilkins [b], Liu Dehan [a], Liu Zufa [a], Fu Jiamu [a]

[a]*State Key Laboratory of Organic Geochemistry, Guangzhou Institute of Geochemistry, Chinese Academy of Sciences, PR China*
[b]*CSIRO Petroleum North Ryde, PO Box 136, NSW 2113, Australia*

Received 10 August 1999; accepted 8 May 2000
(returned to author for revision 2 November 1999)

Abstract

Evaluation of the maturity of Chinese lower Palaeozoic sediments has not been satisfactorily accomplished because of the absence of vitrinite and the relatively high level of maturity of the organic matter. In the Tarim Basin, one of the largest petroliferous basins in China, important lower Palaeozoic marine sediments contain a widely distributed type of maceral resembling vitrinite, especially characterised by syndepositional occurrence, elongate shape, homogenous texture and weak anisotropy. The term vitrinite-like maceral is used to describe the maceral in this paper because of insufficient evidence for its origin. Thirty-five lower Palaeozoic source rocks, mainly from five boreholes in the Tarim Basin, have been investigated by organic petrologic methods and a positive correlation between the vitrinite-like maceral reflectance and sample depth has been recognized. This correlation is better than that between bitumen reflectance and depth. Artificial maturation data show that the maturation pathway of vitrinite-like macerals is quite different from that of vitrinite. There is a distinct step in the development of reflectance of vitrinite-like macerals with increasing maturation. By combining the reflectance data from naturally and artificially matured samples, the relationship between vitrinite-like maceral reflectance and vitrinite reflectance can be divided into three stages which are well-represented by three linear regression equations. The equations provide a convenient method to evaluate the maturity of Lower Palaeozoic sediments by allowing an equivalent vitrinite reflectance to be derived from the measured vitrinite-like maceral reflectance.

Keywords: Lower Palaeozoic; Hydrocarbon source rock; Thermal maturity; Vitrinite reflectance; Bitumen reflectance; Vitrinite-like maceral reflectance

1. Introduction

Lower Palaeozoic hydrocarbon source rocks are of widespread occurrence in some large Palaeozoic petroliferous basins in China. Extensive geochemical studies on the organic matter of these source rocks have been carried out recently, but little work has been done on their thermal maturity using the methods of organic petrography (Xiao, 1992). Consequently, much work is still required before the thermal maturity of lower Palaeozoic source rocks in China can be confidently assessed. There are three reasons for the limited application of organic petrological methods (Xiao et al., 1995; Zhong and Qiu, 1995; Jin, 1997). One is the absence of true vitrinite originating from higher plants, and the second is the relatively high maturity of these source rocks so that many conventional maturity parameters are not suitable. The third reason is the rare occurrence and difficult microscopic differentiation between various zooclasts in these rocks, restricting the application of maturity parameters proposed for lower Palaeozoic

* Corresponding author.
E-mail address: xmxixo@gig.ac.cn (X. Xiao).

0146-6380/00/$ - see front matter
PII: S0146-6380(00)00061-9

source rocks such as the reflectance of chitinozoans, graptolites and scolecodonts (Goodarzi, 1984, 1985; Bertrand and Heroux, 1987; Tricker et al., 1992; Obermajer et al., 1996).

Since 1980, a type of maceral resembling vitrinite has been recognised in the Lower Palaeozoic sediments of several areas (Kisch, 1980; Van Gijzel, 1981; Thomsen et al., 1983; Fowler and Douglas, 1984; Buchardt et al., 1986; Buchardt and Lewan, 1990; Gilkson et al., 1992; Zhong and Qiu, 1995; Jin, 1997; Xiao et al., 1997). The possibility has been discussed that its reflectance could be used as a maturity parameter (Buchardt and Lewan, 1990; Zhong and Qiu, 1995; Xiao et al., 1997). For instance, Buchardt and Lewan (1990) carried out some detailed work on this maceral in the Cambrian-Ordovician Alum Shale of southern Scandinavia. They investigated its response to thermal stress and found a negative correlation between reflectance values and the atomic H/C ratios of the total kerogen.

Two macerals, pyrobitumen and bituminite, can be easily confused with vitrinite-like macerals, and the latter have usually been referred to as pyrobitumen (Bertrand and Heroux, 1987). Along with the refinement of the concept of solid bitumen in sediments (Curiale, 1986), it has been recognised that vitrinite-like macerals are of syndepositional origin and different from any other type of bitumen. The term bituminite has been used for a similar maceral in source rocks by some authors (Teichmuller, 1982, 1986), but this maceral lacks a definite morphology. It occurs in a finely streaky form dispersed amongst minerals (corresponding to amorphinite in kerogen) or as a groundmass for other macerals (Teichmuller, 1982). In addition to morphological differences, the vitrinite-like maceral has a distinctly different origin than bituminite. The source matter of bituminite is in fact a mixture of algae, animal plankton, bacterial lipids and other precursors (Teichmuller, 1982; 1986), but individual particles of vitrinite-like maceral in a source rock were derived from a single source material, although the exact nature of the source material may not be clear (Buchardt and Lewan, 1990; Jin, 1997).

The Tarim Basin, one of the world's largest frontier basins, is dominated by lower Palaeozoic sediments (Kang, 1992). Recently, more than 20 deep wells have been drilled through Cambrian-Ordovician sediments and vitrinite-like macerals have been widely observed in these strata (Jin, 1997; Xiao et al., 1997). However, little work has been done on optical properties related to thermal maturation of this maceral. The primary aim of the present study was to investigate reflectance evolution of vitrinite-like macerals with increasing thermal maturity, and to develop a method which can be conveniently used to rank organic matter from lower Palaeozoic source rocks of the Tarim Basin as well as those from other Chinese petroliferous basins.

2. Samples and methods

About one hundred lower Palaeozoic core samples collected from 10 boreholes in the Tarim Basin were examined by microscopy. From these, a total of 35 samples were selected from five boreholes for reflectance measurements (Fig. 1 and Table 1). These samples are all of Cambrian-Ordovician age, mainly with TOC's ranging from 0.30 to 2.50%, and most contain vitrinite-like macerals as well as bitumen. Available data including Rock-Eval analysis of whole rocks and geochemical parameters from GC–MS analysis of extracted saturated hydrocarbons suggest that there is a simple downhole pattern of increasing maturation with depth, and the maturation levels of these samples are from mature to overmature.

The measurement of reflectance was made on polished resin-embedded whole rock blocks with a Leica MPV3 photomicroscope. Polarized reflected light was used to measure the mean random percentage reflectance in oil. The reflectances of vitrinite, vitrinite-like macerals, and bitumen were abbreviated as %VRo, %VLMRo and %BRo, respectively. Data were deleted if there were less than 15 individual measurements on each type of organic matter for a sample, or if the standard deviation for a range of *Ro* was over 0.10% ($Ro < 1.0\%$), 0.15% ($Ro = 1.0–3.0\%$) and 0.20% ($Ro > 3.0\%$).

For comparison with natural thermally matured samples, two Carboniferous marine source rocks of low maturity from the Tarim Basin well Ba4 (Fig. 1) were artificially matured to different maturity levels during programmed pyrolysis experiments. Tables 1 and 2 present some geological and geochemical data for the two samples. Sample TT-1 contains vitrinite as well as vitrinite-like macerals, but vitrinite is rare in sample TT-2. A humic coal of Permian age from the Datong coal mine in Sanxi province of north China, with 0.61% VRo (that is with the same reflectance as the indigenous vitrinite in sample TT-1), was added to sample TT-2 in an amount of 3–5 wt.% for the experiments, in order to rank the organic matter of the samples. The dominant maceral of the kerogen from both samples is micrinite with a lower reflectance, ranging 0.50–0.55%. This maceral is the product of thermal maturation of humic amorphinite (Xiao et al., 1997). The artificial maturation experiments were carried out in a closed vacuum steel autoclave without added water. About 100 g of sample crushed to 0.10–0.20 mm was used in each heating experiment. Samples were heated isothermally for 50 h at temperatures between 200 and 500°C. At the conclusion of the runs, the kerogens were isolated from the two sets of samples, made into resin-embedded blocks and polished. Reflectance for both vitrinite-like macerals and vitrinite were measured in the same way as that described for the naturally matured samples.

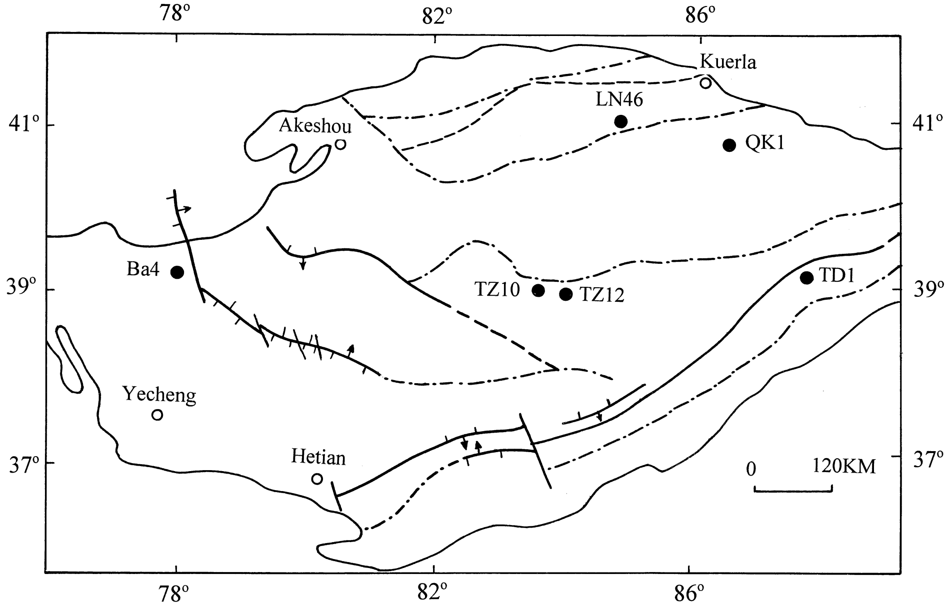

Fig. 1. Map showing locations of the studied wells in the Tarim Basin. Two low maturity Carboniferous samples from well Ba4 were used for the thermal simulation studies.

3. Results and discussion

3.1. Organic petrology of vitrinite-like macerals

Organic clasts are common in the lower Palaeozoic hydrocarbon source rocks of the Tarim Basin. They are of diverse origin and include bitumen, vitrinite-like macerals, chitinozoans, graptolites, scolecodonts and other zooclasts. The concept of vitrinite-like macerals is not well-defined: however, the organic clasts defined as vitrinite-like macerals in this paper do not include any bitumen and have the following characteristics:

1. In reflected light they are dark grey to greyish white, depending on maturity, with a great range in outline, such as elongate, irregular lenticular, angular or rounded, and in general similar to the vitrinite-like macerals described by Buchardt and Lewan (1990) and Stasiuk (1994). However, elongate and irregularly shaped lenses with lengths of 20–150 μm, paralleling the bedding plane, predominate in the Tarim Basin samples. Vitrinite-like macerals generally have a smooth homogenous surface without internal structures even at high maturation levels. In some cases (Fig. 2), some highly reflecting pyrite grains are included.
2. Vitrinite-like macerals have a dark brown fluorescence induced by blue light, and an obvious positive alteration in source rocks of low maturity. The fluorescence intensity decreases with increasing maturity and the extinction of visible fluorescence occurs at about 0.50–0.60% VLMRo.
3. Vitrinite-like macerals develop a weak anisotropy with increasing maturation. Bireflectance is easily measured where the reflectance exceeds 1.50% and ranges 0.20–0.80% for the studied samples.
4. Vitrinite-like macerals occur widely in marine strata, especially in organic-rich argillaceous limestones and shales with kerogen of type II. In most cases, it is the dominant form of organic matter except for amorphinite or micrinite.

On the basis of the above description, vitrinite-like macerals can be most easily identified in whole rock blocks. They are distinguished from zooclasts by their typically elongate shape and uniform reflectance, and from bitumen by their syndepositional occurrence, weak anisotropy and homogenous texture (Table 3, and Fig. 2).

A reasonable explanation of the origin of vitrinite-like macerals should include two aspects: source material and the process of formation. Several possible sources have been mentioned in the literature. They are: (1) the polysaccharides of graptolites and chitinozons (Goodarzi, 1984, 1985); (2) the polysaccharides of multicellular algal seaweeds, fungal hyphae, and arthropod cuticle (Buchardt and Lewan, 1990); (3) degradation products of algae (Glikson and Taylor, 1986; Goodarzi et al., 1992; Jin, 1997). As it appears that humification can occur in marine environments (Romankerich, 1984), the

Table 1
Geological and some Rock–Eval data for samples from Tarim Basin wells

Sample no.	Well	Depth (m)	Age[a]	Lithology	TOC (%)	T_{max} (°C)	S_1 (mg/g)	S_2 (mg/g)	HI (mg/g. TOC)
TD1-6	TD1	2275	O_{2+3}	Gray mudstone					
TD1-7	TD1	2893	O_{2+3}	Dark gray mudstone	0.30	/[b]	0.01	0.02	7
TD1-8	TD1	3172	O_{2+3}	Dark gray mudstone					
TD1-10	TD1	3588	O_{2+3}	Black gray mudstone					
TD1-11	TD1	3841	O_{2+3}	Black gray mudstone					
TD1-13	TD1	4154	O_{2+3}	Dark gray mudstone	1.04	/	0.0	0.10	11
TD1-15	TD1	4360	O_1	Black gray mudstone	2.31	513	0.0	0.23	10
TD1-16	TD1	4661	O_1	Black mudstone	5.03	530	0.10	0.32	6
TD1-19	TD1	4801	∈	Gray limestone					
QK1-2	QK1	2486	O_{2+3}	Dark gray silt mudstone					
QK1-4	QK1	2716	O_{2+3}	Dark gray silt mudstone					
QK1-5	QK1	3012	O_{2+3}	Dark mudstone					
QK1-10	QK1	3350	O_{2+3}	Dark gray mudstone					
QK1-11	QK1	3710	O_{2+3}	Black gray mudstone	0.24	/	0.01	0.02	9
QK1-19	QK1	4013	O_{2+3}	Black gray mudstone	0.28	/	0.02	0.02	7
QK1-22	QK1	4333	O_{2+3}	Dark gray mudstone					
QK1-23	QK1	4507	O_{2+3}	Black gray mudstone					
LN46-1	LN46	4773	C	Gray silt mudstone					
LN46-4	LN46	5207	C	Dark gray limestone					
LN46-5	LN46	5535	S	Dark gray silt mudstone					
LN46-6	LN46	5569	O_{2+3}	Dark gray argillaceous limestone					
LN46-10	LN46	5830	O_{2+3}	Dark argillaceous limestone					
LN46-11	LN46	5835	O_{2+3}	Dark argillaceous limestone					
LN46-14	LN46	5916	O_{2+3}	Dark argillaceous limestone	0.32	/	0.0	0.02	10
LN46-15	LN46	5919	O_{2+3}	Dark gray argillaceous limestone					
LN46-19	LN46	6036	O_{2+3}	Dark gray argillaceous limestone					
LN46-24	LN46	6090	O_1	Dark gray argillaceous limestone	0.30	/	0.02	0.04	30
LN46-26	LN46	6169	O_1	Dark gray argillaceous limestone					
TZ12-4	TZ12	4004	C	Dark gray silt mudstone					
TZ12-7	TZ12	4669	O_{2+3}	Dark gray argillaceous limestone	0.36	442	0.08	0.53	142
TZ12-10	TZ12	4806	O_{2+3}	Dark gray argillaceous limestone	0.68	444	0.14	1.10	162
TZ12-11	TZ12	4970	O_{2+3}	Dark gray argillaceous limestone	1.50	448	0.39	1.68	1.80
TZ12-13	TZ12	5075	O_{2+3}	Dark gray argillaceous limestone	1.18	446	0.21	0.80	68
TZ12-15	TZ12	5109	O_{2+3}	Dark gray argillaceous limestone					
TZ12-19	TZ12	5291	O_1	Dark gray mudstone					
TZ10-2	TZ10	4461	O_{2+3}	Dark gray argillaceous limestone					
TZ10-4	TZ10	4920	O_{2+3}	Dark gray argillaceous limestone	1.05	443	0.08	0.43	41
TZ10-7	TZ10	5243	O_{2+3}	Dark gray argillaceous limestone	0.49	448	0.03	0.36	74
TT1	Ba4	2023	C	Dark gray mudstone	1.04	440	0.10	0.81	78
TT2	Ba4	2041	C	Dark gray limestone	0.68	439	0.06	0.71	104
DT1	Datong mine		P	Humic coal	79.48	438	12.13	124.78	157

[a] P, Permian; C, Carboniferous; S, Silurian: O_1, lower Ordovician; $O_{2\text{-}3}$, upper-middle Ordovician; ∈, Cambrian.
[b] S_2 peak too low to determine a reasonable value of T_{max}.

Table 2
Maceral analysis and vitrinite reflectance values of samples used for thermal simulation experiments

Sample	Well	Basin	Depth (m)	Age[d]	Lithology	VRo (%)	V[a] (%)	VLM[a] (%)	I[a] (%)	E[a] (%)
TT-1	Ba4	Tarim	2023	C	Dark gray mudstone	0.61	4.65	5.99	75.77[b]	13.59
TT-2	Ba4	Tarim	2041	C	Dark gray limestone	/[c]	0.53	21.96	71.56[b]	5.86
DT1		Datong mine		P	Coal	0.61	83.45	0.0	6.05	10.50

[a] Volume percentages: V, vitrinite; VLM- vitrinite-like maceral; I, inertinite; E, exinite.
[b] Micrinite, derived from humic amorphinite.
[c] Insufficient vitrinite for reflectance measurement.
[d] C, Carboniferous, P, Permian.

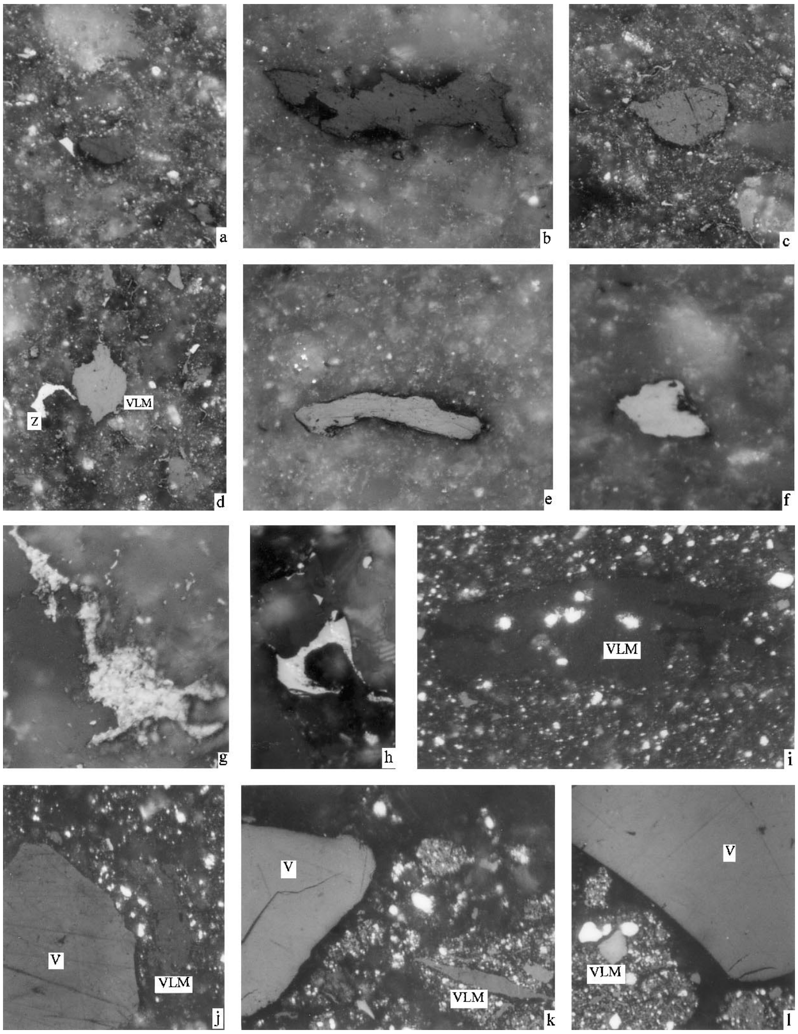

Fig. 2. Vitrinite-like macerals and bitumen with different maturities from whole rocks (a–h) and kerogens (i–l) of the Tarim Basin. The sample numbers are the same as in Table 1. Reflected light ×460. (a) Vitrinite-like maceral Ro% = 0.64, TZ12-7; (b) vitrinite-like maceral Ro% = 0.78, TZ10-4; (c) vitrinite-like maceral Ro% = 1.02, LN46-11; (d) vitrinite-like maceral (VLM) Ro% = 1.45 and zooclast (z), QK1-22; (e) vitrinite-like maceral Ro% = 2.08, TD1-8; (f) vitrinite-like maceral Ro% = 3.02, TD1-16; (g) bitumen Ro% = 2.48, TD1-10; (h) bitumen Ro% = 3.30, TD1-13; (i) vitrinite-like maceral(VLM) Ro% = 0.30, containing pyrite grains, TT2 (j) vitrinite-like maceral (VLM) and vitrinite (V) from the added coal, unheated sample TT-2; (k) vitrinite-like maceral (VLM) and vitrinite (V) from the added coal, TT2 heated to 340°C; (l) vitrinite-like maceral (VLM) with a stronger reflectance than the vitrinite (V) from the added coal, TT2 heated to 400°C.

vitrinite-like macerals were presumably formed by a process of gelification of polysaccharides of diverse origins (Buchardt and Lewan, 1990).

While the origin of the Tarim Basin vitrinite-like macerals is still a matter for further investigation, the studies mentioned above give some indications of a possible origin. It seems most likely that the vitrinite-like macerals in the Tarim Basin formed mainly by the gelification of organic matter related to algae. There are three lines of evidence: (1) The rocks containing the vitrinite-like macerals formed in an open carbonate shelf facies in which gelification could take place. (2) In some rocks of Ordovician age of low maturity, vitrinite-like macerals have a very low reflectance, only a little higher than exinite at the same rank. This shows that the source material of the macerals is rich in hydrogen. (3) The outline and size of the vitrinite-like macerals are similar to multicellular algae.

3.2. Reflectance relationships between macerals

As different types of zooclasts are not easily distinguished in the source rocks of the Tarim Basin (Jin, 1997), the measurements of reflectance were made only

Table 3
Comparison of criteria for microscopic identification of vitrinite-like macerals and bitumen in Cambrian–Ordovician strata of the Tarim Basin

Marker	Bitumen	Vitrinite-like maceral
Occurrence	Filling pores and fissures, perpendicular or crossing bedding planes	Syndepositional, paralleling bedding planes
Outline	Indefinite, depending on the shape of pores and fissures	Typically elongate, irregular lenses
Optical properties	With optical texture, such as grained mosaic, small domain, and strong anisotropy at higher stages of maturity	Homogenous texture, with weak anisotropy
Mineral inclusion	Without mineral inclusions	Sometimes with pyrite grains
Origin	Secondary solid bitumen	Original maceral

Table 4
Measured reflectance results for samples from Tarim Basin wells

Sample no.	Well	Depth (m)	Age[a]	Vitrinite-like maceral		Bitumen	
				Ro (%)[c]	S.D.[d]	Ro (%)[c]	S.D.[d]
TD1-6	TD1	2275	O_{2+3}	1.93–2.45/2.130 (25)	0.08	2.13–2.78/2.41 (15)	0.09
TD1-7	TD1	2893	O_{2+3}	2.04–2.60/2.25 (30)	0.12	2.00–2.80/2.51 (23)	0.08
TD1-8	TD1	3172	O_{2+3}	1.99–2.64/2.35 (25)	0.06	2.11–3.10/2.73 (18)	0.10
TD1-10	TD1	3588	O_{2+3}	2.14–2.85/2.65 (38)	0.08	2.48–3.30/2.92 (17)	0.08
TD1-11	TD1	3841	O_{2+3}	2.32–3.12/2.91 (15)	0.10	2.72–3.65/3.20 (28)	0.12
TD1-13	TD1	4154	O_{2+3}	2.85–3.29/3.04 (15)	0.03	3.02–3.88/3.45 (35)	0.17
TD1-15	TD1	4360	O_1	2.86–3.72/3.14 (20)	0.18	3.12–4.28/3.82 (27)	0.10
TD1-16	TD1	4661	O_1	2.72–3.24/3.21 (27)	0.08	3.54–4.37/4.07 (28)	0.11
TD1-19	TD1	4801	∈	3.01–3.85/3.40 (27)	0.10	4.20–4.88/4.57 (15)	0.06
QK1-2	QK1	2486	O_{2+3}	0.82–1.02/0.98 (24)	0.03	n/f[e]	
QK1-4	QK1	2716	O_{2+3}	0.88–1.24/1.13 (24)	0.03	1.28–1.64/1.44 (20)	0.03
QK1-5	QK1	3012	O_{2+3}	0.99–1.38/1.21 (26)	0.04	1.20–1.69/1.52 (20)	0.06
QK1-10	QK1	3350	O_{2+3}	1.04–1.40/1.28(20)	0.03	n/f	
QK1-11	QK1	3710	O_{2+3}	1.30–1.68/1.43 (15)	0.02	1.24–1/70/1.54 (21)	0.06
QK1-19	QK1	4013	O_{2+3}	1.11–1.69/1.40 (21)	0.06	1.32–1.83/1.68 (24)	0.04
QK1-22	QK1	4333	O_{2+3}	1.24–1.69/1.55 (21)	0.04	1.38–1.88/1.72 (18)	0.04
QK1-23	QK1	4507	O_{2+3}	1.30–1.62/1.43 (18)	0.02	1.64–2.31/1.92 (24)	0.05
LN46-1	LN46	4773	C	0.76–0.99/0.92 (18)[b]	0.04	n/f	
LN46-4	LN46	5207	C	0.91–1.10/0.98[b]	0.02	n/f	
LN46-5	LN46	5535	S	0.76–0.87/0.79 (16)	0.08	0.78–1.01/0.91 (15)	0.04
LN46-6	LN46	5569	O_{2+3}	0.78–0.98/0.85 (24)	0.04	n/f	
LN46-10	LN46	5830	O_{2+3}	0.82–1.04/0.92 (20)	0.03	1.11–1.39/1.30 (16)	0.04
LN46-11	LN46	5835	O_{2+3}	0.90–1.12/0.98 (20)	0.05	1.02–1.43/1.29 (25)	0.03
LN46-14	LN46	5916	O_{2+3}	0.98–1.16/1.02 (18)	0.02	1.23–1.64/1.44 (20)	0.04
LN46-15	LN46	5919	O_{2+3}	0.98–1.39/1.09 (24)	0.04	1.18–1.64/1.50 (20)	0.06
LN46-19	LN46	6036	O_{2+3}	1.00–1.28/1.12 (23)	0.03	n/f	
LN46-24	LN46	6090	O_1	1.10–1.40/1.24 (17)	0.02	1.27–1.88/1.65 (20)	0.04
LN46-26	LN46	6169	O_1	1.08–1.43/1.28 (23)	0.04	1.33–1.88/1.78 (24)	0.03
TZ12-4	TZ12	4004	C	0.64–0.82/0.71 (23)[b]	0.02	n/f	
TZ12-7	TZ12	4669	O_{2+3}	0.57–0.78/0.63 (24)	0.02	0.53–0.58/0.55 (15)	0.01
TZ12-10	TZ12	4806	O_{2+3}	0.58–0.75/0.65 (24)	0.02	0.45–0.52/0.50 (15)	0.01
TZ12-11	TZ12	4970	O_{2+3}	0.60–0.76/0.69 (15)	0.03	0.58-0.67/0.61 (15)	0.01
TZ12-13	TZ12	5075	O_{2+3}	0.64–0.90/0.79 (15)	0.04	n/f	
TZ12-15	TZ12	5109	O_{2+3}	0.68–0.95/0.81 (17)	0.04	n/f	
TZ12-19	TZ12	5291	O_1	0.74–1.00/0.82 (20)	0.08	0.68-0.94/0.87 (20)	0.03
TZ10-2	TZ10	4461	O_{2+3}	0.63–0.85/0.72 (23)	0.03	0.60-0.78/0.74 (15)	0.08
TZ10-4	TZ10	4920	O_{2+3}	0.65–0.95/0.84 (18)	0.02	0.60-0.77/0.71 (19)	0.04
TZ10-7	TZ10	5243	O_{2+3}	0.73–1.10/0.96 (19)	0.03	0.60-0.78/0.68 (15)	0.05

[a] C, Carboniferous; S, Silurian; O_1, lower Ordovician; $O_{2\text{-}3}$, upper-middle Ordovician; ∈, Cambrian.
[b] Vitrinite reflectance.
[c] Max-min/average (number of measured points).
[d] S.D., standard deviation.
[e] n/f, not found.

for bitumens of characteristic occurrence in pores and fissures, and vitrinite-like macerals with well-defined features (Fig. 2). Since bitumen develops a grained mosaic optical texture at higher stages of maturity in the Tarim Basin, a larger measured field was used in order to obtain a stable mean reflectance. Three major observations can be made from the data presented in Table 4 and Fig. 3.

1. VLMRo ranges from 0.63 to 3.40% for the studied samples. There is a positive correlation between VLMRo and depth for each of the wells. For wells TD1 and QK1 where the samples have a higher maturity, this relationship is nearly linear, and the correlation is better than for wells LN46 and TZ12 in which the organic matter has lower maturity.
2. There is also a positive correlation between BRo and depth for each of the wells similar to that observed by Jacob (1985). This correlation is nearly linear except for well TZ12.
3. The reflectance of vitrinite-like macerals for most samples is quite different from that of the asso-

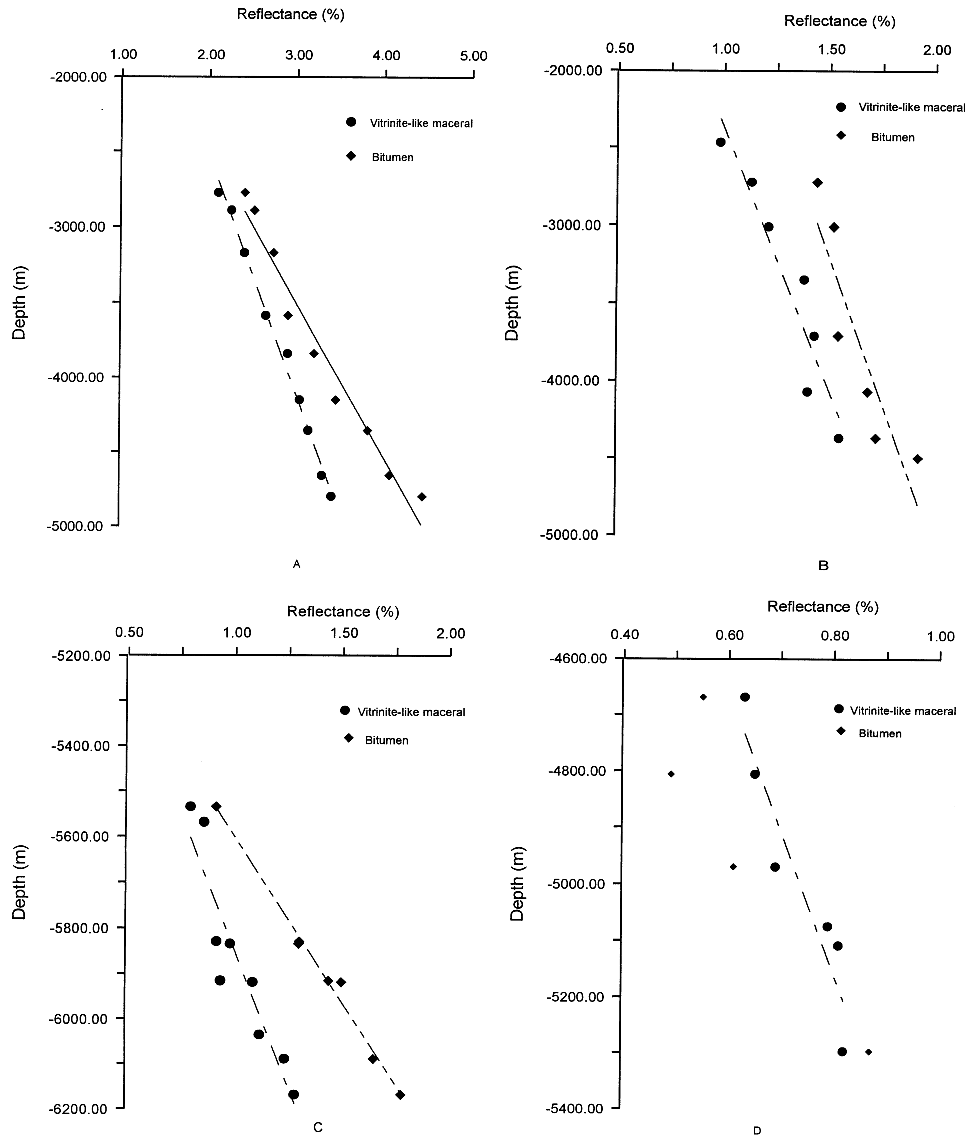

Fig. 3. Scatter diagrams of reflectance values of vitrinite-like maceral and bitumen against depth for (A) well TD1; (B) well QK1 ; (C) well LN46 and (D) well TZ12.

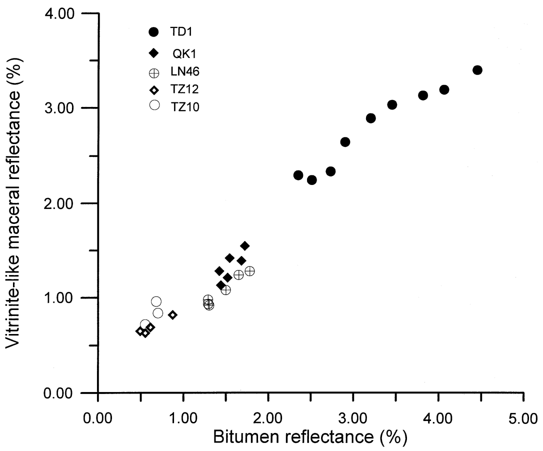

Fig. 4. Relationship between vitrinite-like maceral reflectance and bitumen reflectance for naturally matured samples from the Tarim Basin. Data from Table 2.

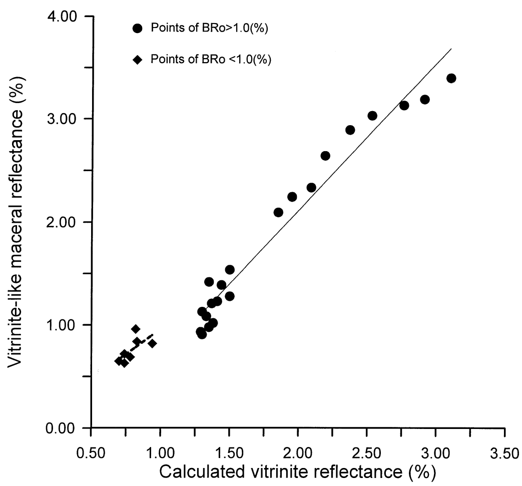

Fig. 5. Relationship between vitrinite-like maceral reflectance and the equivalent vitrinite reflectance of Cambrian- Ordovician source rocks from the Tarim Basin. The equivalent vitrinite reflectance is derived from Jacob's (1985) equation relating solid bitumen random reflectance to vitrinite reflectance.

ciated bitumen. VLMRo is lower than BRo for samples from all the wells except TZ12, where the maturity of the source rocks is relatively low (BRo < 1.0%).

The correlation between VLMRo and depth is better than that between BRo and depth, with regression coefficients $r^2 = 0.90$–0.95 and 0.75–0.90 respectively.

Consequently, the reflectance of vitrinite-like macerals may be used as a thermal maturation indicator for lower Palaeozoic source rocks in the Tarim Basin, and is an even more reliable indicator than the reflectance of solid bitumen. Fig. 4 presents the relationship between VLMRo and BRo for the studied samples, and it demonstrates that there is no simple linear relationship throughout the maturation range studied, similar to that noted by Riediger (1993) between bitumen reflectance and T_{max}. There are two equations available for the relationship between solid bitumen reflectance and vitrinite reflectance from which measured BRo can be transformed into equivalent VRo: = 0.618 BRo + 0.40 (Jacob, 1985) and VRo% = 0.66BRo + 0.34 (Liu and Shi, 1994). There are only small differences (0.06–0.11%) between values of VRo calculated from the two equations through the maturity range of the studied samples. The relationship between VLMRo and calculated VRo based on Jacob' s equation is shown in Fig. 5. The data are separated into two groups by a gap occurring at about 0.70–1.0% VLMRo. For VRo > 1.0%, the relationship between VRo and VLMRo is nearly linear. For VRo < 1.0%, the data points have greater deviation. There are two possible reasons:

(1) Jacob 's equation is not suitable for lower maturity samples. Xiao et al. (1995) applied a thermal simulation experiment to investigate the reflectance evolution of bitumen with increasing maturation and found that a nearly linear relationship between the reflectance of bitumen and vitrinite occurs only for VRo = 1.0–3.0%.
(2) There is no simple linear relationship between VLMRo and VRo for the studied samples. Compared with vitrinites, vitrinite-like macerals are relatively rich in hydrogen, which has a significant effect on the maturation patterns of macerals. For instance, the coalification path of alginite is marked by jumps (Glikson et al., 1992; Stasiuk, 1994); the reflectance evolution of sporinite and cutinite with increasing maturation is similar to that of bitumen, showing slow changes up to 1.0% VRo, followed by a rapid rise after the oil window (Xiao et al., 1997). Buchardt and Lewan (1990) found the maturation pathway of their vitrinite-like macerals was different from that of vitrinite, but quite similar to that of "suppressed" vitrinite.

For these reasons, more data are required to understand the relationship between VLMRo and VRo in the lower range of maturity. For the present, it is of critical importance to establish a direct correlation between the reflectance values of vitrinite-like macerals and vitrinite in samples from the basin under study. As noted above, the maturity of lower Palaeozoic source rocks in the Tarim Basin is generally relatively high, mostly with an equivalent VRo > 1.0% (Xiao et al., 1996; Jin, 1997),

Table 5
Measured reflectances of artificially matured samples

Temperature (°C)	Sample TT1 VRo(%)[a]	Sample TT1 VLMRo(%)[a]	Sample TT2 VRo(%) of the added coal[a]	Sample TT2 VLMRo(%)[a]
Original sample	0.54–0.66/0.61 (0.03)	0.31–0.33/0.32 (0.01)	0.60–0.62/0.61 (0.01)	0.29–0.30/0.30 (0.01)
200	0.52–0.70/0.63 (0.02)	0.30–0.33/0.32 (0.01)	0.60–0.63/0.62 (0.01)	0.31–0.32/0.31 (0.01)
250	0.53–0.71/0.69 (0.03)	0.38–0.46/0.42 (0.01)	0.61–0.73/0.71 (0.01)	0.36–0.42/0.40 (0.01)
280	0.74–0.93/0.88 (0.02)	0.44–0.53/0.51 (0.02)	0.81–0.92/0.89 (0.01)	0.47–0.60/0.57 (0.02)
310	1.08–1.38/1.15 (0.02)	0.63–0.81/0.74 (0.02)	0.98–1.11/1.09 (0.01)	0.64–0.70/0.68 (0.01)
340	1.26–1.43/1.38 (0.01)	0.84–0.98/0.91 (0.02)	1.20–1.41/1.37 (0.02)	0.78–0.90/0.85 (0.02)
370	1.34–1.67/1.54 (0.02)[b]		1.26–1.48/1.42 (0.02)	1.11–1.34/1.23 (0.02)
400	1.58–1.97/ 1.78 (0.04)[b]		1.54–1.89/1.72 (0.02)	1.63–1.97/1.80 (0.04)
450	2.18–2.87/2.49 (0.05)[b]		2.03–2.53/2.25 (0.02)	2,30–2.86/2.54 (0.05)
500	2.64–3.38/2.95 (0.12)[b]		2.48–2.84/2.67 (0.02)	2.85–3.56/3.14 (0.06)

[a] Max-min/average (standard deviation). The measured points range from 25 to 35.
[b] Reflectance values of the mixture of vitrinite-like macerals and vitrinite.

that is, in the range where a strong relationship exists between VLMRo and VRo. The reflectance evolution pathway of vitrinite-like macerals at lower maturation levels would be best evaluated mainly from artificial thermal maturation data.

3.3. Artificial thermal simulation pathway of the vitrinite-like maceral

Table 5 presents the measured reflectance values of the artificially matured samples. The microscopic differentiation between vitrinite-like maceral and vitrinite in sample TT-1 disappears gradually with increasing pyrolysis temperature and it is difficult to discriminate between them in samples heated to 370°C and above. For this reason, the measured reflectance values for sample TT-1 heated above 370°C were obtained from the mixture of vitrinite and vitrinite-like macerals. The vitrinite reflectance values for sample TT-2 obtained from the added humic coal can be used to rank the organic matter for both samples. As shown in Fig. 6, the maturation pathway of vitrinite is different from that of the vitrinite-like maceral. The positive correlation between VRo and the pyrolysis temperature is nearly linear, but for VLMRo there was a very slow rise in the range of 200–370°C, followed by a rapid increase at higher temperature. Whereas the reflectance values of the vitrinite-like maceral become even higher than those of vitrinite after 370°C, it is noteworthy that vitrinite-like macerals have a very low reflectance in the early stages of maturation. For example, at VRo = 0.65–0.70%, VLMRo is 0.30–0.40% (Table 5), a little higher than that of the liptinite (0.15–0.20%) of the added coal. A possible and direct explanation for this is that the source material of the vitrinite-like macerals was rich in hydrogen, and totally different from the organic matter from which vitrinite forms. Fig. 7 presents the relationship between VLMRo and VRo for the artificially matured samples. The curve may be conveniently divided into three sections by the trends representing three evolutionary stages of the vitrinite-like macerals during thermal maturation.

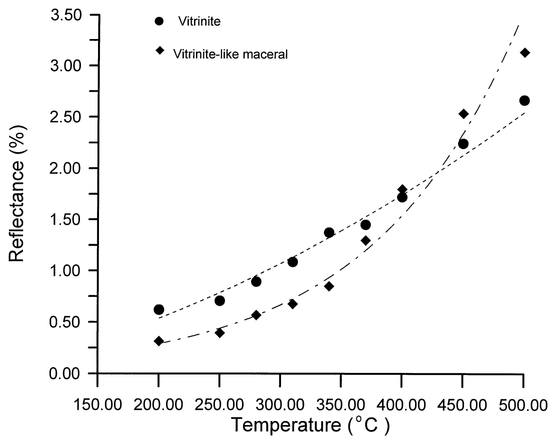

Fig. 6. Artificial maturation pathway of vitrinite and vitrinite-like macerals with increasing temperature. The pyrolysis time for all experiments was 50h. The maturation path of the vitrinite-like maceral is marked by a jump in the range of 0.75–1.50% VLMRo in contrast to the more regularly increasing path of vitrinite.

Stage 1: VLMRo increases very slowly with increasing VRo where VLMRo < 0.75%.

Stage 2: A sharp increase of VLMRo occurs in the range 0.75–1.50% VLMRo, corresponding to the oil window of the vitrinite-like macerals (Xiao et al., 1997).

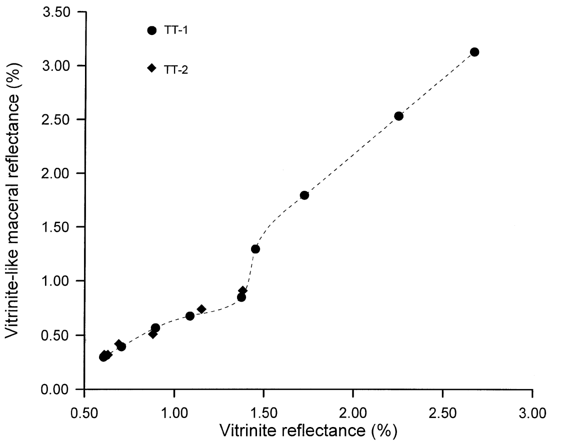

Fig. 7. Correlation between vitrinite-like maceral reflectance and vitrinite reflectance for artificially matured samples with increasing maturation. The curve can be divided into three stages: VLMRo < 0.75%; 0.75–1.50% and > 1.50%.

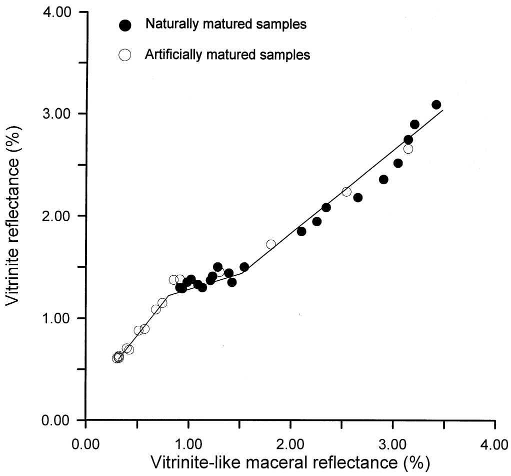

Fig. 8. Correlation between VLMRo and VRo based on natural and artificially matured samples. Results with BRo < 1.0% for natural samples were deleted.

Stage 3: VLMRo increases steadily with increasing VRo where VLMRo = 1.50–3.0% VLMRo.

It should be noted that although the factors controlling thermal maturation of organic matter for naturally and artificially matured samples are totally different, the relationship between VLMRo and VRo for both sets of samples is comparable. One of the primary aims of this study was to develop equations describing the relationship between VLMRo and VRo that could be used to evaluate the maturity of Lower Palaeozoic source rocks. The above data confirm the pattern of evolution indicated by the natural samples.

3.4. *Evaluation of maturity of lower Palaeozoic source rocks*

Fig. 8 presents the relationship between VLMRo and VRo from both naturally and artificially matured samples. The good coincidence of the two sets of data confirms that data from artificial samples can also be an aid in ranking the maturity of source rocks. The three stages discussed above (between VLMRo and VRo) are also recognized in the combined data of Fig. 8. They are well-represented by three linear regression equations:

$$\text{Stage I: VRo\%} = 1.26\ \text{VLMRo} + 0.21 \quad (\text{VLMRo} < 0.75\%)$$

$$\text{Stage II: VRo\%} = 0.28\ \text{VLMRo} + 1.03 \quad (\text{VLMRo} = 0.75-1.50\%)$$

$$\text{Stage III: VRo\%} = 0.81\ \text{VLMRo} + 0.18 \quad (\text{VLMRo} > 1.50\%)$$

The three equations make it possible to obtain an equivalent vitrinite reflectance from a measured vitrinite-like maceral reflectance, and to evaluate indirectly the maturity of lower Palaeozoic source rocks. According to this approach, the equivalent VRo and maturation levels of the lower Palaeozoic source rocks from the studied wells in the Tarim Basin are:

(1) The Cambrian–Ordovician source rocks from well TD 1: 1.90–2.90% VRo; dry gas stage.
(2) The Ordovician source rocks from well QK1: 1.20–1.50% VRo; wet gas stage.
(3) The Ordovician source rocks from well LN46: 1.10–1.40% VRo; late oil generation and wet gas stage.
(4) The Ordovician source rocks from wells TZ12 and TZ10: 1.0–1.20% VRo; oil generation peak to late oil generation stages.

4. Conclusions

A systematic study of the morphological and optical properties of vitrinite-like macerals in the Tarim Basin indicates the following.

1. Vitrinite-like macerals are of widespread occurrence in the Lower Palaeozoic source rocks of the Tarim Basin. They are syndepositional, typically characterized by an elongate shape parallel to bedding, a uniform texture and weak anisotropy.
2. The data from natural evolutionary sequences and artificial maturation experiments show that vitrinite-like maceral reflectance can be used as a maturity index. The correlation between VLMRo

and VRo can be well represented by three linear equations corresponding to three maturity stages: VRo% = 1.26 VLMRo + 0.21 (VLMRo < 0.75%); VRo% = 0.28 VLMRo + 1.03 (VLMRo = 0.75–1.50%); and VRo% = 0.81 VLMRo + 0.18 (VLMRo > 1.50%).

3. The corresponding equivalent VRo values of Cambrian-Ordovician source rocks from the studied wells in the Tarim Basin are 1.90–2.90% for TD1; 1.20–1.50% for QK1; 1.10–1.40% for LN46; and 1.10–1.20% for TZ12 and TZ10. Consequently the Cambrian-Ordovician source rocks of the Tarim Basin are mostly in the late oil generation to overmature stages.

Acknowledgements

We would like to express our great gratitude to Dr. L. D. Stasiuk, Dr. M. Fowler and an anonymous reviewer for their helpful criticism and suggestions. We also extend our thanks to the Office of Project 96-101 for permission to publish the data. This research has been supported by the project Studies of Petroleum Pool Geochemistry of the Lunan Oilfield, Tarim Basin (001106) and the project Fundamental Geochemical Problems in Petroleum System (KZ951-B1-412).

Associate Editor—**M. Fowler**

References

Bertrand, B., Heroux, Y., 1987. Chitinozoan, graptolite, and scolecodont reflectance as an alternative to vitrinite and pyrobitumen reflectance in Ordovician and Silurian strata, Anticosti Island, Quebec, Canada. American Association of Petroleum Geologists Bulletin 71, 951–957.

Buchardt, B., Clausen, J., Thomsen, E., 1986. Carbon isotope composition of lower Palaeozoic kerogen: effects of maturation. Organic Geochemistry 10, 127–134.

Buchardt, B., Lewan, M.D., 1990. Reflectance of vitrinite-like macerals as a thermal maturity index for Cambrian–Ordovician Alum Shale, southern Scandinavia. American Association of Petroleum Geologists Bulletin 74, 394–406.

Curiale, J.A., 1986. Origin of solid bitumens, with emphasis on biological marker results. Organic Geochemistry 10, 559–580.

Fowler, M.G., Douglas, A.G., 1984. Distribution and structure of hydrocarbons in four organic-rich Ordovician rocks. Organic Geochemistry 6, 105–114.

Glikson, M., Taylor, G.H., 1986. Cyanobacterial mats as major contributors to organic matter in the Toolebuc oil shales. Geological Society of Australia Special Publication 12, 273–286.

Glikson, M., Taylor, D., Morris, D., 1992. Lower Palaeozoic and Precambrian petroleum source rocks and the coalification path of alginite. Organic Geochemistry 18, 881–897.

Goodarzi, F., 1984. Organic petrology of graptolite fragments from Turkey. Marine and Petroleum Geology 1, 202–210.

Goodarzi, F., 1985. Reflected light microscopy of chitinozoan fragments. Marine and Petrology Geology 2, 72–78.

Goodarzi, F., Fowler, M.G., Bustin, M., McKirdy, D.M., 1992. Thermal maturity of early Palaeozoic sediments as determined by their optical properties of marine-derived organic matter–a review. In: Schidlowski, M., Golubic, S., Kimberly, M.M., McKirdy, D.M., Trudinger, P.A. (Eds.), Early Organic Evolution: Implications for Mineral and Energy Resources. Springer-Verlag, Berlin, pp. 270–295.

Jacob, H., 1985. Disperse solid bitumens as an indicator for migration and maturity in prospecting for oil and gas. Erdöl und Kohle 38, 365–366.

Jin Kuili, (Ed.), 1997. Organic Petrology — A Case Study of Tarim Basin. Seismic Press, Beijing, pp. 118–130 (in Chinese).

Kang, Y. Z. 1992. Oil and gas fields of Palaeozoic age in the Tarim Basin. Press of China University of Geoscience, Beijing, pp. 1–78. (in Chinese).

Kisch, H.J., 1980. Incipient metamorphism of Cambro-Silurian clastic rocks from the Jaamtland Supergroup, Central Scandinavian Caledonides, western Sweden: illite crystallinity and "vitrinite" reflectance. Journal of the Geological Society of London 137, 271–288.

Liu, D.H., Shi, J.Y., 1994. Evaluation of early Palaeozoic carbonate source rocks. Natural Gas Industry 14 (6), 32–36 (in Chinese).

Obermajer, M., Fowler, M.G., Goodarzi, F., Snowdon, L.R., 1996. Assessing thermal maturity of Palaeozoic rocks from reflectance of chitinozoa as constrained by geochemical indicators: an example from southern Ontario. Canada Marine and Petroleum Geology 13, 907–920.

Riediger, L.L., 1993. Solid bitumen reflectance and Rock-Eval Tmax as maturation indices: an example from the "Nordegg Member", Western Canada Sedimentary Basin. International Journal of Coal Geology 22, 295–315.

Romankerich, E. A., 1984. Geochemistry of Organic Matter in the Ocean. Springer-Verlag, Berlin.

Stasiuk, L.D., 1994. Oil-prone alginite macerals from organic-rich Mesozoic and Palaeozoic strata Saskatchewan, Canada. Marine and Petroleum Geology 11, 208–218.

Teichmüller, M., 1982. Origin of the petrographic constituents of coal. In: Stach, E., Mackowsky, M.-Th., Teichmüller, M., Taylor, G.H., Chandra, D., Teichmüller, R. (Eds.), Stach's Textbook of Coal Petrology. Gebrüder Borntraeger. Stuttgart, Berlin, pp. 269–271.

Teichmüller, M., 1986. Organic petrology of source rocks, history and state of the art. Organic Geochemistry 10, 581–599.

Thomsen, E., Lindgreen, H., Wrang, P., 1983. Investigation on the source rock potential in Denmark. Geologie en Mijnbouw 62, 221–239.

Tricker, P.M., Marshall, J.E.A., Badman, T.D., 1992. Chitinozoan reflectance: a lower Paleozoic thermal maturity indicator. Marine and Petroleum Geology 9, 302–307.

Van Gijzel, P., 1992. Applications of the geomicrophotometry of kerogen, solid hydrocarbons and crude oils to petroleum exploration. In: Brooks, J. (Ed.), Organic Maturation Studies and Fossil Fuel Exploration. Academic Press, London, pp. 351–377.

Xiao Xianming (Ed.), 1992. Organic Petrology and its Application to Petroleum Exploration, Guangdong Scientific Press. Guangzhou, pp. 55–98 (in Chinese).

Xiao Xianming, Wu Zhijin, Liu Dehan, 1995. Evaluation of maturation level of lower Palaeozoic strata. Acta Sedimentol. Sinica 13, 112–119 (in Chinese).

Xiao, X., Liu, D., Fu, J., 1996. Multiple phases of hydrocarbon generation and migration in the Tazhong petroleum system of the Tarim Basin, People's Republic of China. Organic Geochemistry 25, 191–197.

Xiao Xianming, Liu Dehan, Fu Jiamo, 1997. Marine vitrinite-an important hydrocarbon source matter in marine source rocks. Acta Petrolei Sinica 18, 44–49 (in Chinese).

Zhong, N. N., Qiu,Y. (Eds.), 1995. Organic Petrology of Carbonate Rocks. Scientific Press, Beijing, pp. 20–30, 58–65 (in Chinese).